Research Article

Zhenghao Zhang, Xin Shen, Yingyi Zhang*, Guangqiang Zhang, Zhaohui Xie, and Zhichen Han

Effects of hydrothermal carbonization process parameters on phase composition and the microstructure of corn stalk hydrochars

https://doi.org/10.1515/htmp-2025-0079
received October 27, 2024; accepted May 04, 2025

Abstract: The steel metallurgy industry is a high energy consuming and high polluting industry. In order to reduce the consumption of fossil fuels such as coke and coal powder and environmental pollution, it is urgent to develop a new type of clean energy for green metallurgy. Biomass straw energy, as a renewable and clean energy source, has attracted widespread attention from metallurgical researchers. In this work, the corn stalk hydrochars were prepared by hydrothermal carbonization (HTC) method at different carbonization temperatures, carbonization times, and mass ratios, aiming to provide a green and sustainable energy source for the metallurgical industry. In addition, the influences of parameter changes on phase composition, microstructure, and calorific value were also analyzed. Results manifested that the elevation of temperature and time promoted the HTC process, contrary to the solid–liquid proportion. It was worth noting that short carbonization time and high mass ratios were unconducive to the dissolution of harmful phase KCl, which affected the application of hydrochar. Under the optimal carbon process conditions (T = 260°C, t = 40 min, S/L = 2%), the corn stalk hydrochar has a smaller particle size (<50 μm), higher calorific value (22.34 MJ·kg^{-1}), and carbon content (76.46 wt%), which has a great potential to replace anthracite and promote the sustainable development of the metallurgical industry.

Keywords: hydrothermal carbonization, phase composition, microstructure, corn stalk hydrochars.

*** Corresponding author: Yingyi Zhang,** School of Metallurgical Engineering, Anhui University of Technology, Maanshan, 243002, Anhui, China, e-mail: zhangyingyi@ahut.edu.cn, tel: +86 17375076451
Zhenghao Zhang: School of Metallurgical Engineering, Anhui University of Technology, Maanshan, 243002, Anhui, China; Shanghai Meishan Iron and Steel Limited by Share Ltd, Nanjing, 210039, Jiangsu, China
Xin Shen, Zhichen Han: School of Metallurgical Engineering, Anhui University of Technology, Maanshan, 243002, Anhui, China
Guangqiang Zhang, Zhaohui Xie: Shanghai Meishan Iron and Steel Limited by Share Ltd, Nanjing, 210039, Jiangsu, China

1 Introduction

Biomass energy is the only renewable carbon-based energy source in nature, which has the advantage of zero carbon dioxide emissions and is an ideal alternative to traditional fossil energy [1]. As a major agricultural industry country, China has abundant biomass resources of crop straw. China's straw resources are mainly composed of rice, corn, and wheat straw, which account for about 75% of the total straw production in the country [2]. However, the sharp increase in crop solid waste production has brought serious management problems to the agricultural sector [3,4]. At present, most of the straw biomass resources are directly burned because direct combustion is the cheapest and most convenient treatment method. Although direct incineration improves the utilization rate of straw to a certain extent, there are many disadvantages and negative effects in terms of environmental protection. For example, emissions of CO_2, CO, NO_X, and SO_2 from crop burning contribute to global warming and atmospheric pollution. Among them, carbon dioxide contributes about 60% to the greenhouse effect [5,6]. In addition, the smoke particles generated by crop burning can also lead to a decrease in air quality and visibility, and cause acute and chronic respiratory diseases in humans [7,8]. Polycyclic aromatic hydrocarbons (PAHs) are carcinogenic pollutants [2], which are mainly byproducts of the incomplete combustion of fossil fuels and biomass. Zhang et al. [7] tested the PAHs after burning various stalks, and found that the emission factors of rice and corn stalks were 5.26 and 1.74 mg·kg^{-1}, respectively. Therefore, straw burning seriously affects human life and threatens human health, which deserves more attention [3,8–10]. If biomass fuels are used instead of fossil fuels in the metallurgical industry, it can not only save a lot of fossil energy and solve the carbon emissions problem of fossil fuels, but also avoid environmental pollution caused by direct combustion of biomass fuels. Because various emission reduction and dust removal measures in the metallurgical industry can

effectively alleviate the pollution caused by direct combustion of biomass fuels.

The rapid growth of biomass straw resources is both an opportunity and a challenge for various countries [11,12]. Biomass straw can be enhanced in value through various technological combinations, and through thermochemical treatment, biomass straw can be converted into energy intensive intermediate products. However, converting biomass residue into energy materials that can replace traditional fuels without drying remains an urgent obstacle that needs to be overcome [13,14]. HTC has great potential to convert wet biomass residues into carbon rich high-value products. In this process, water is mainly used as a solvent, and dehydration and decarboxylation reactions are carried out at relatively mild temperatures and self-pressures, resulting in liquid phases rich in organic compounds and solid phases rich in hydrochars [13,15–17]. In addition, the application of HTC technology in biomass treatment has received more and more attention [12,13,18–20]. Zhang et al. [21] optimized the coal like granulation process using wheat straw as fuel, and concluded that the scheme optimized by HTC parameters and granulation process could produce wheat straw hydrochar pellets with similar production capacity to lignite and better fuel characteristics than mother pellets. The higher heating value increased from 19.6 to 27.9 $MJ \cdot kg^{-1}$ for hydrochar pellets. Kambo and Dutta [22] reviewed the basic principles and reaction mechanisms of slow pyrolysis and HTC processes, compared the advantages and disadvantages of the two processes, and pointed out that hydrochar is a valuable resource with less alkali metal content and higher calorific value than biochar. Libra et al. [16] believed that hydrothermal carbon has opened up the field of carbon production from non-traditional renewable waste, which can be applied to a wide range of fields according to demand. Sharma et al. [23] reviewed the application of HTC in various industries and believed that HTC process is the best coalification process. Although HTC process can realize clean and efficient utilization of biomass straw, the effects of HTC process on the phase composition, surface functional groups, microstructure and heating value evolution of corn stalk hydrochars are still unclear.

In this work, the corn stalk biomass resources were utilized to fabricate renewable hydrochar by the HTC process. The effects of HTC parameters on phase composition, surface functional groups, and microstructure evolution of the corn stalk hydrochars were measured and analyzed. In addition, the influence of carbonization process parameters on the calorific values of corn stalk hydrochars has also been investigated.

2 Experimental procedure

2.1 Preparation of corn stalk hydrochars

The mechanical stirring high-pressure reactor (TGYF-0.25) was used to prepare hydrothermal carbon from corn stalk biomass. First, the dried corn stalks were crushed into biomass particles with a size less than 10 mm, and then put into a high-pressure reactor for a single factor HTC experiment with a carbonization pressure of 5 MPa, as shown in Figure 1. The solid–liquid mass ratios, time, and temperature were 1–4%, 20–80 min, and 180–300°C, respectively. After carbonization, the corn stalk hydrochars filtered using filter paper were dried in an electric hot air-drying oven at a temperature and time of 105°C and 3 h, respectively. Finally, the HTC

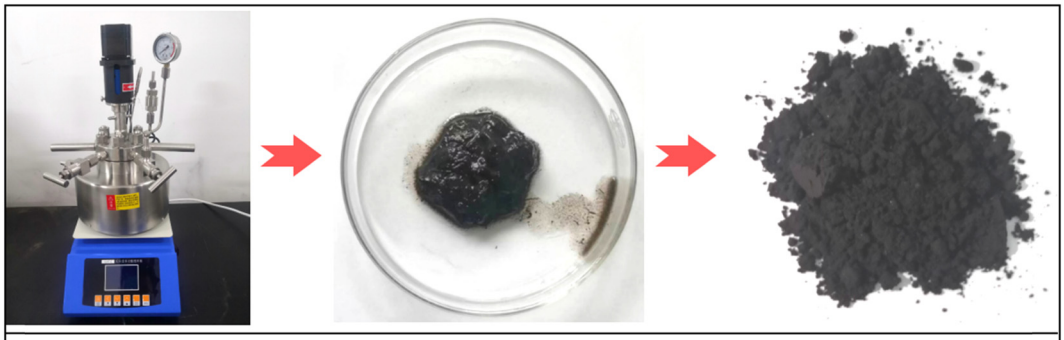

Carbonization equipment and parameters

Carbonization equipment	Pressure	Temperature	Time	S/L ratio
Electric blast drying oven	5 MPa	180-300°C	20-80 min	1-4%

Figure 1: Experimental device and process parameters of HTC.

method was used to prepare corn stalk hydrochars at different carbonization temperatures (180, 220, 260, and 300°C), carbonization times (20, 40, 60, and 80 min), and mass ratios (*S*/*L*, 1, 2, 3, and 4%). The corn stalk hydrochars prepared under various HTC process conditions were annotated as HTC180 (t = 40 min, *S*/*L* = 2%), HTC220 (t = 40 min, *S*/*L* = 2%), HTC260 (t = 40 min, *S*/*L* = 2%), HTC300 (t = 40 min, *S*/*L* = 2%), HTC20 (T = 260°C, *S*/*L* = 2%), HTC40 (T = 260°C, *S*/*L* = 2%), HTC60 (T = 260°C, *S*/*L* = 2%), HTC80 (T = 260°C, *S*/*L* = 2%), HTC1 (t = 40 min, T = 260°C), HTC2 (t = 40 min, T = 260°C), HTC3 (t = 40 min, T = 260°C), and HTC4 (t = 40 min, T = 260°C), respectively.

2.2 Testing techniques

The phase component of the hydrochars after HTC of corn stalk were identified using X-ray diffractometer (XRD, Miniflex 600, Rigaku) with Cu radiation (Cu-Kα, λ = 1.5406 A), scanning rate of 5°/min and 2θ angle of 10–90°. The scanning electron microscopy (SEM-EDS, JSM-6510LV, JEOL) coupled with an X-ray energy dispersive spectrometer was adopted to analyze the surface structure and elemental composition of hydrochars. In order to increase the conductivity of hydrochars, an ion sputtering instrument (SBC-12) was used for surface coating of hydrochars. The sputtering target material was a gold target, and the sputtering current and time were 6 mA and 30 s, respectively. The sputtered samples were used for SEM surface morphology and elemental analysis at an acceleration voltage of 20 kV and a detector current of 60 mA. The Fourier transform infrared spectrometer (FTIR, Thermo Scientific Nicolet 10, America) of hydrochars under different process conditions were recorded by spectrograph (VERTEX 70, Bruker), and the 256 scans were recorded from the wavenumber range of 500–4,000 cm^{-1} with the resolution of 4 cm^{-1}. In addition, the fully automatic calorimeter (ZDHW-2B) was used to test the calorific value of the corn stalk hydrochars at an ignition voltage of 24 V and an ignition time of 6 min, and the test standard was in accordance with GB/T213-2008 standard.

3 Results and discussion

3.1 Phase composition evolution of the maize stalk hydrochars

3.1.1 Effect of the carbonization temperature

Figure 2 presents the XRD patterns of corn stalk hydrochars prepared at various carbonization temperatures. When the carbonization temperature is in the lower range

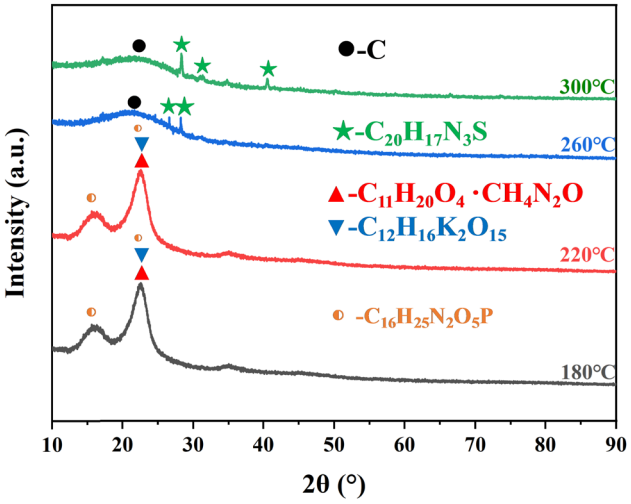

Figure 2: XRD patterns of corn stalk hydrochars prepared at 180–300°C.

(180–220°C), the hydrochars of corn stalk are mainly composed of Undecanedioic acid urea ($C_{11}H_{20}O_4{\cdot}CH_4N_2O$, 22.78°), potassium hydrogen trilactate ($C_{12}H_{16}K_2O_{15}$, 22.73°), and *N*-isopropyl aminocarbonyl methoxy *N* (benzyl ethoxycarbonyl methyl) phosphamide ($C_{16}H_{25}N_2O_5P$, diffraction angles are 22.70° and 16.20°, respectively). When the carbonization temperature rises to 260–300°C, the carbonized products are transformed into cyano-2-(4-dimethylaminophenyl)-[1-(4-phenyl)-2-thiazolyl] ethylene ($C_{20}H_{17}N_3S$, 26.728° and 28.358°) and amorphous carbon (21.178°). In addition, increasing the carbonization temperature can significantly increase the carbon content of maize stalk hydrochars and reduce the oxygen content. When the carbonization temperature increased from 180 to 300°C, the carbon content of maize stalk hydrochars increased from 48.12 to 69.13 wt%, while the oxygen content decreased from 35.31 to 15.7 wt% [4]. The chemical analysis also showed that the sulfur content of hydrochars also increased slightly with the increasing carbonization temperature (0.31–0.86 wt%), which is consistent with the analysis results of XRD. Therefore, raising the carbonization temperature will promote the dehydration and dehydroxylation reaction of corn stalk, and promote the carbonization reaction.

3.1.2 Effect of the carbonization time

Figure 3 displays the XRD patterns of corn stalk hydrochars prepared at 20–80 min. It can be observed that the product of corn stalk hydrochars is very complicated at a carbonization time of 20 min, mainly composed of poly[(–)-anti-head-to-head coumarin dimer 1,6-hexandiamide] ($C_{24}H_{28}N_2O_4$, 22.549° and 28.218°), poly [alanyl triglycine) hydrate] ($C_9H_{16}N_4O_5$), 1,7-Dinaphthylthiocarbazone ($C_{21}H_{16}N_4S$, 29.555°), 3-Azido-1,2,4-

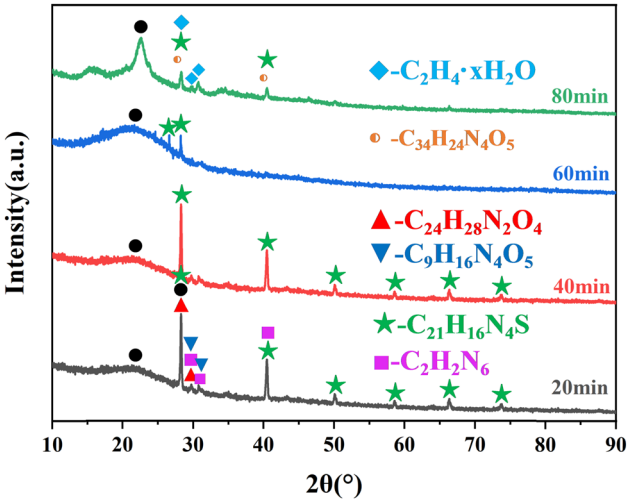

Figure 3: XRD patterns of corn stalk hydrochars prepared at 20–80 min.

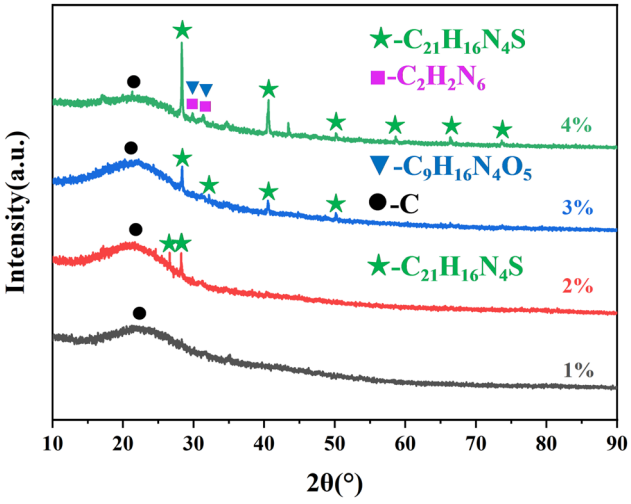

Figure 4: XRD patterns of corn stalk hydrochars prepared at the mass ratios of 1–4%.

triazole ($C_2H_2N_6$, 28.795°, 31.254° and 40.946°) and a small amount of amorphous carbon (21.178°). After increasing the carbonization time to 40 min, the carbonized products are mainly composed of 1,7-Dinaphthylthiocarbazone ($C_{21}H_{16}N_4S$, 29.555°) and a small amount of amorphous carbon (21.178°). When the carbonization time is 60 min, the diffraction peak quantity and intensity of 1,7-Dinaphthylthiocarbazone ($C_{21}H_{16}N_4S$, 29.555°) phase decrease significantly, while the peak intensity of amorphous carbon (21.178°) increases significantly. When the carbonization time is 80 min, the diffraction peak intensity of 1,7-Dinaphthylthiocarbazone ($C_{21}H_{16}N_4S$, 29.555°) phase slightly decreased. Meanwhile, a high carbon content of poly paraphthaloyl chloride *p*-phenylenediamine 3,4′ diaminodiphenyl ether ($C_{34}H_{24}N_4O_5$, 29.679° and 42.174°) and ethylene hydrate ($C_2H_4 \cdot xH_2O$, 27.769°, 30.624° and 34.129°) phases are also observed. In addition, an obvious carbon diffraction peak is also observed at the position of 21.178°. The chemical element analysis also showed that increasing the carbonization time can significantly increase the carbon content of maize stalk hydrochars and reduce the oxygen content. When the carbonization time increased from 20 to 80 min, the carbon content of maize stalk hydrochars increased from 52.27 to 69.05 wt%, while the oxygen content decreased from 30.30 to 13.58 wt% [4]. The above results indicate that increasing the carbonization time can significantly improve the carbonization effect of corn straw and promote the dehydration and decarboxylation reactions of HTC.

3.1.3 Effect of mass ratios

The XRD patterns of corn stalk hydrochars prepared at various solid–liquid mass ratio are presented in Figure 4. When the mass ratio is 1%, the carbonized product is almost completely carbonized into amorphous carbon. In addition to amorphous carbon, small amounts of 1,7-Dinaphthylthiocarbazone ($C_{21}H_{16}N_4S$, 29.555°) is also observed at solid–liquid mass ratio of 2 and 3%. When the solid–liquid mass ratio reaches 4%, the diffraction peak intensity of amorphous carbon decreased significantly, while the diffraction peak quantity and intensity of 1,7-Dinaphthylthiocarbazone ($C_{21}H_{16}N_4S$) increased observably, with the diffraction peaks at 28.309°, 40.510°, 50.167°, 58.642°, 66.123°, and 73.729°, respectively. In addition, small amounts of poly [alanyl triglycine) hydrate] ($C_9H_{16}N_4O_5$, 26.914° and 29.555°) and 3-azide-1,2,4-triazole ($C_2H_2N_6$, 28.795° and 31.254°). The chemical element analysis also showed that increasing the mass ratio can slightly decrease the carbon content of maize stalk hydrochars and slightly increase the oxygen content. When the carbonization time increased from 1 to 4%, the carbon content of maize stalk hydrochars decreased from 67.15 to 66.02 wt%, while the oxygen content decreased from 16.81 to 17.41 wt% [4]. Therefore, the lower the solid–liquid mass ratio, the better the carbonization effect, and the lower solid–liquid proportion can facilitate the dehydration and dehydroxylation reaction of corn stalk. From the perspective of production efficiency, while the solid–liquid mass ratio is 2–3%, HTC can ensure both a better carbonization effect and a higher production efficiency.

3.2 Surface functional groups of the maize stalk hydrochars

3.2.1 Effect of the carbonization temperature

Figure 5 presents the FTIR patterns of corn stalk hydrochars prepared at various carbonization temperatures.

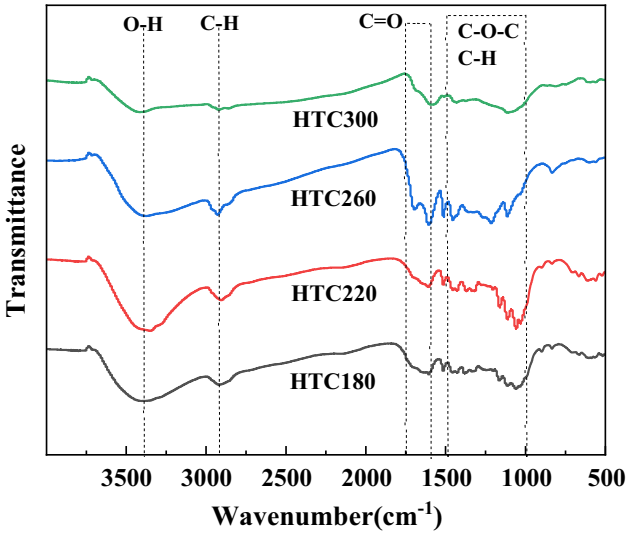

Figure 5: FTIR patterns of corn stalk hydrochars prepared at different carbonization temperatures.

It can be found from Figure 5 that there is a very wide absorption peak at 3,406 cm^{-1}, which corresponds to the stretching vibration absorption peak of the hydroxyl group (−OH). The interaction between alcohol and hydrogen bonds produces water, which leads to the loss of hydroxyl group, and the peak intensity decreases with increasing temperature [24]. The results reveal that there is an obvious intermolecular or intramolecular dehydration reaction between cellulose and hemicellulose when the carbonization temperature increased. The stretching vibration absorption peaks of C–H bonds of aliphatic hydrocarbon or cycloalkane are observed at the wave number of 2,930 cm^{-1}, and the peak intensity gradually decreases with the increase in temperature, indicating that no demethylation reaction occurs at a low carbonization temperature, and the $-CH_3$ and $-CH_2$ on the biomass are relatively stable [25]. The expansion vibration absorption peaks of C═O bond are observed at the wave number of 1,750 and 1,610 cm^{-1}, and the intensity of the absorption peaks decreases with increasing carbonization temperature. The stretching vibration peaks of C–O–C and C–H bonds are between 1,030 and 1,505 cm^{-1}, and the two bonds are relatively stable. Therefore, the spectrograms of the two bonds change similarly when the temperature changes.

3.2.2 Effect of the carbonization time

Figure 6 presents the FTIR patterns of corn stalk hydrochars prepared at various carbonization times. There are wide hydroxyl (−OH) stretching vibration absorption peaks in both time and temperature samples near 3,400 cm^{-1}, and the corresponding peak intensity decreases with the increase in time. The deformation vibrations at 2,800–3,000 cm^{-1} and 1,300–1,498 cm^{-1} indicate the presence of alkanes, and the peak intensity does not change significantly with increasing time, which indicates that demethylation reaction is not easy to occur at lower temperatures. The stretching vibration of the C–O bond is observed near 1,610 cm^{-1}, which indicates the bending mode of the absorbed water [26]. It can be seen that the intensity of the absorption peak decreases gradually with the increase in time, which indicates that the corn stalk hydrochar has good hydrophobicity. Therefore, the longer the carbonization time, the better the carbonization effect.

3.2.3 Effect of the mass ratios

Figure 7 presents the FTIR patterns of corn stalk hydrochars prepared at various mass ratios. It can be seen that a wide spectral band is formed near the center of 3,400 cm^{-1}, which is due to the intermolecular or intramolecular dehydration reaction between cellulose and hemicellulose. Strong hydrogen bonds formed between liquid water molecules, resulting in the overlap of asymmetric and symmetric stretching vibrations of water [24]. This indicates that the peak intensity of hydroxyl groups gradually decreases with the increase in solid–liquid mass ratios. The stretching vibration absorption peaks of C–H bond in aliphatic hydrocarbon or cycloalkane are observed at 2,919 cm^{-1} [27], and the peak strength did not change significantly with the increase in solid–liquid mass ratios. The peaks of acids, alcohols, esters, and carboxyl groups

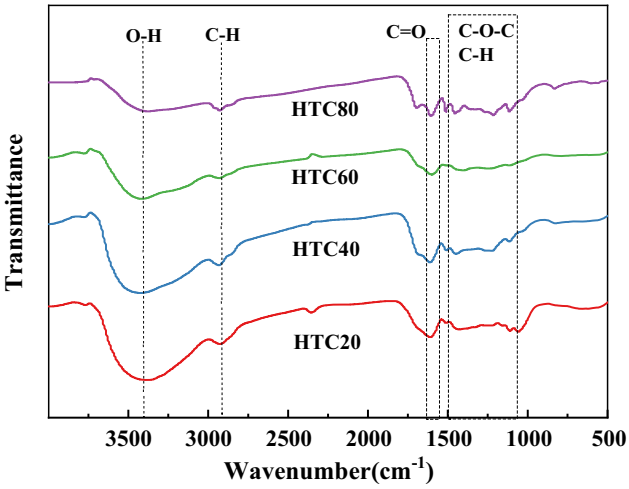

Figure 6: FTIR patterns of corn stalk hydrochars prepared at various carbonization times.

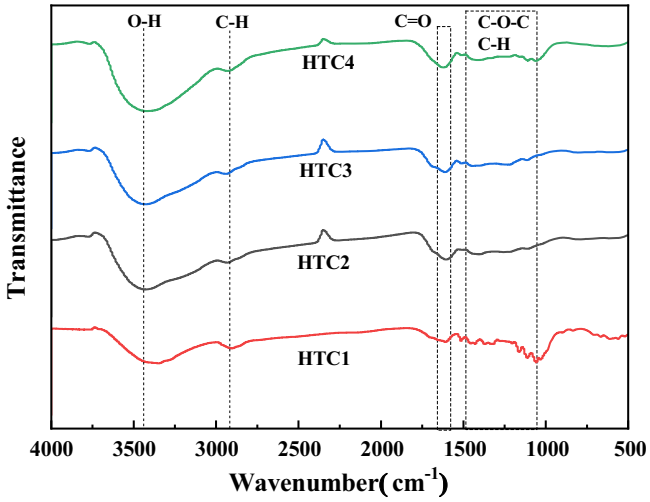

Figure 7: FTIR patterns of corn stalk hydrochars prepared at various solid–liquid mass ratios.

produced by hemicellulose are reduced and shifted within the range of 1,000–1,500 cm^{-1} during carbonization, which indicate that carbonization contributes to the degradation of these hemicellulose compounds. Therefore, the lower the solid–liquid mass ratios, the better the carbonization effect.

3.3 Microstructure evolution of the maize stalk hydrochars

3.3.1 Effect of the carbonization temperature

The SEM images of corn stalk carbonization products prepared at various HTC temperatures are illustrated in Figure 8, and the chemical composition of hydrochar prepared at different carbonization temperatures is shown in Figure 9(a). The SEM-EDS results indicate that the HTC temperature has a significant effect on the microstructure and elemental composition of maize stalk hydrochars. The greater the carbonization temperature, the smaller the particle size of the carbonized products. In addition, the C element increases sharply with the increase in HTC temperature, while the O element is the opposite. This indicates that raising the HTC temperature significantly promotes the dehydrogenation and dehydroxylation reactions of corn stalks, accelerates the decomposition of organic matter, and facilitates the rate of HTC. When the HTC temperature is 180°C, the particle size of corn stem water charcoal is relatively large, and the stripe structure before carbonization can be clearly observed, and the internal cell wall is obviously broken, as shown in Figure 8(a)–(c). The EDS results show that when the carbonization temperature is 180°C, the C and O contents of hydrochars are 52.175 and 47.825 wt%, respectively. Under the HTC temperature of 220°C, the stripe structure of the hydrochar is significantly damaged, and the carbonization products suffered significant agglomeration, as shown in Figure 8(d)–(f). When the HTC temperature increases to 220°C, the C content of hydrochars slightly increases and the O content slightly decreases. The carbon content and oxygen content of hydrochars are 56.54 and 44.46 wt%, respectively. When the carbonization temperature is 260–300°C, the corn stalk is decomposed into small size particles (0.2–2 μm) and long fine particles and long strips (20–50 μm), and the particle size of some carbonized products is only sub-micron. The EDS results show that when the HTC temperature is 260–300°C, the C content increases significantly (71.96–74.36 wt%), while the O content decreases significantly (25.64–28.04 wt%). Increasing the carbonization temperature can significantly improve the carbonization effect.

The calorific values of corn stalk hydrochars prepared at various carbonization temperatures are shown in Figure 9(b). It can be seen that the calorific value of uncarbonized corn stalk is only 16.25 $MJ{\cdot}kg^{-1}$, and increasing carbonization can significantly improve the calorific value of corn stalk hydrochars. Under the carbonization temperature of 260–300°C, the calorific value of corn stalk hydrochars is similar to that of anthracite. The carbon content has a direct effect on the calorific value and combustion properties of hydrochars [30]. The maximum carbon content and calorific value of corn stalk hydrochars are obtained at a carbonization temperature of 300°C, and the maximum carbon content and calorific value are 73.61wt% and 23.58 $MJ{\cdot}kg^{-1}$, respectively. This is very close to the calorific value (24.60 $MJ{\cdot}kg^{-1}$) of anthracite reported by Zhang et al. [31]. The corn stalks contain a large amount of hemicellulose, cellulose, lignin, and

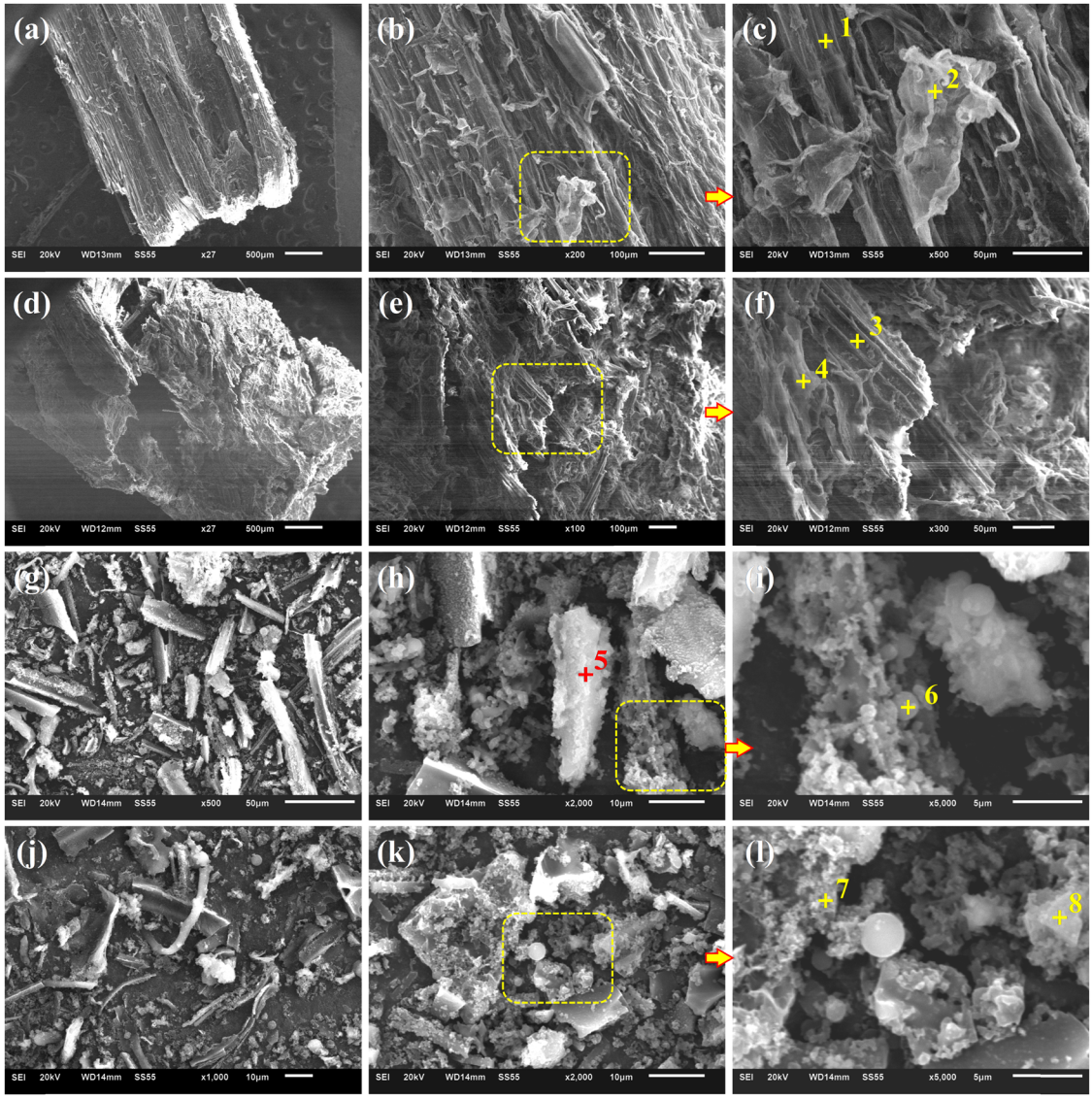

Figure 8: SEM micrographs of corn stalk hydrochars prepared at various carbonization temperatures. (a)–(c) 180°C; (d) and (e) 220°C; (g)–(i) 260°C; and (j)–(l) 300°C.

other components, such as C–HN–HO–H, C–NC═CC–C, C═O, C–O [28]. These chemical bonds will be broken during the HTC process, which has a positive influence on the increase in biomass fuel calorific value [29]. Therefore, increasing the carbonization temperature can significantly increase in the carbon content and calorific value of hydrochars. The corn stalk hydrochars prepared at 260–300°C has a carbon content and calorific value close to anthracite.

3.3.2 Effect of the carbonization time

Figure 10 presents the SEM images of corn stalk hydrochars prepared at various carbonization times, and the corresponding EDS element concentrations are shown in Figure 11(a). The SEM-EDS results indicate that carbonization time has a significant impact on the microstructure and chemical composition of corn stalk hydrochars. It can be seen from Figure 10(a)–(c) that the original structure of corn straw is obviously destroyed under the carbonization time of 20 min, the particle size of corn stalk hydrochars is larger, and some fine white particles with a particle size of about 2–10 μm are also observed. The EDS results show that the white particle phase is KCl, and the element contents of Cl and K are 49.16 and 50.84%, respectively. When the carbonization time increases to 40–80 min, corn stalk hydrochars are decomposed into fine particles and strips. The particle size of the long strip hydrochars is about 10–30 μm, and the particle size

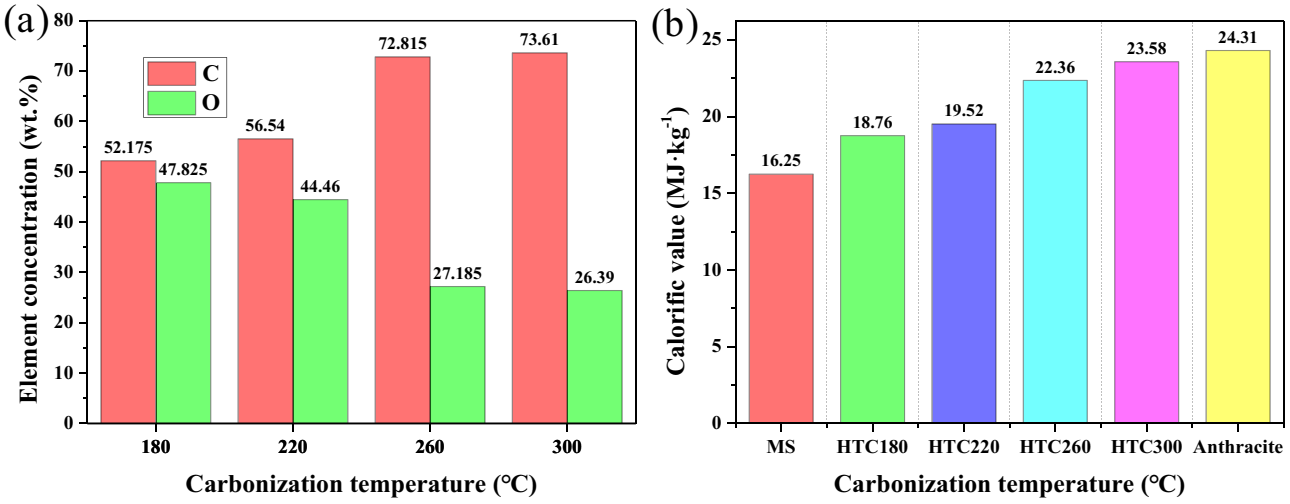

Figure 9: EDS element concentration (a) and calorific value (b) of corn stalk hydrochars prepared at various carbonization temperatures.

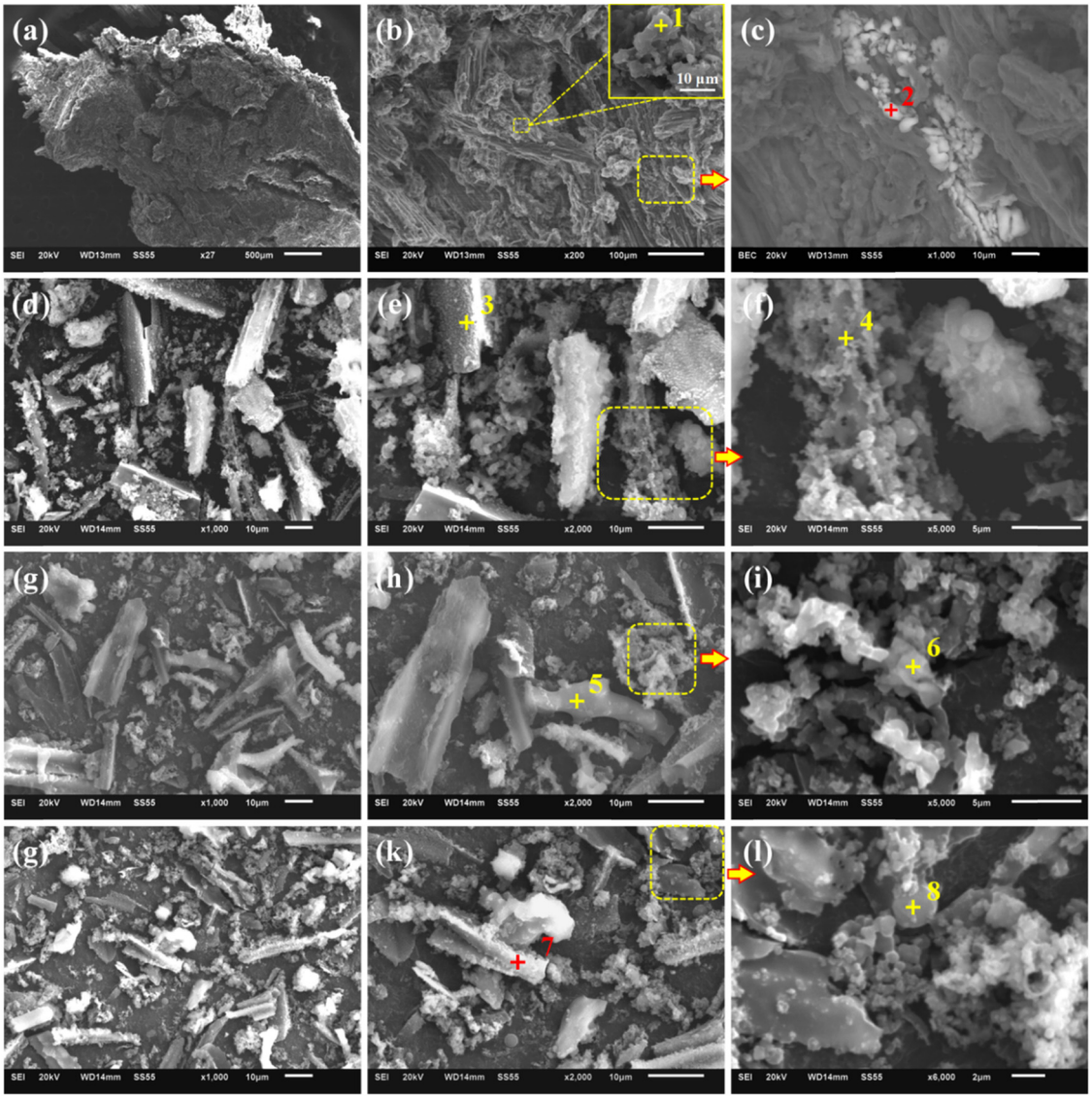

Figure 10: SEM micrographs of corn stalk hydrochars prepared at various carbonization times. (a)–(c) 20 min; (d) and (e) 40 min; (g)–(i) 60 min; and (j)–(l) 80 min.

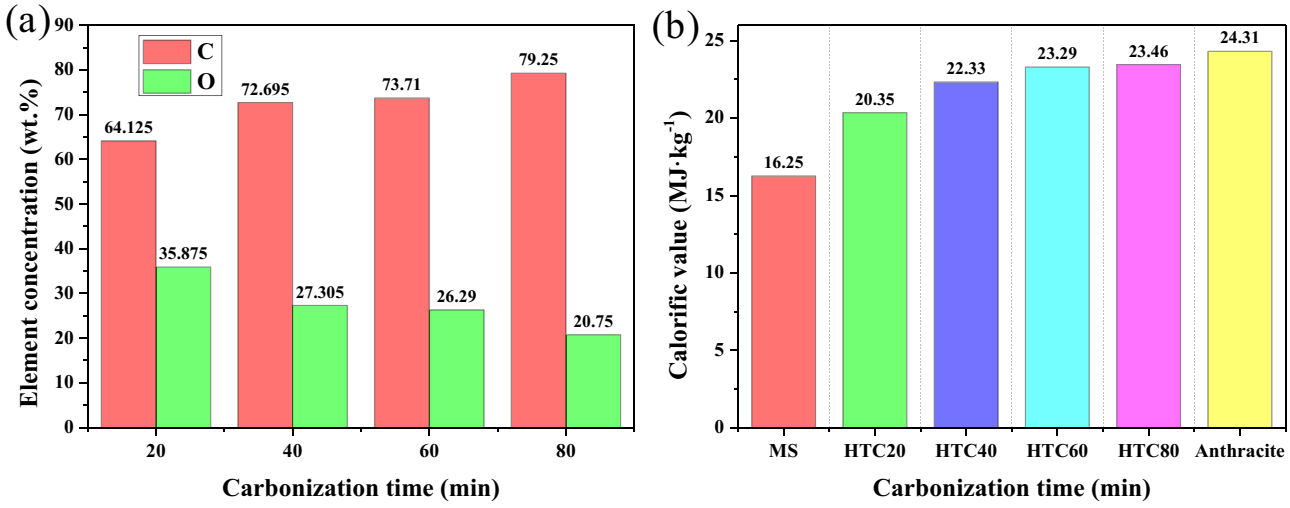

Figure 11: EDS element concentration (a) and calorific value (b) of corn stalk hydrochars prepared at various carbonization times.

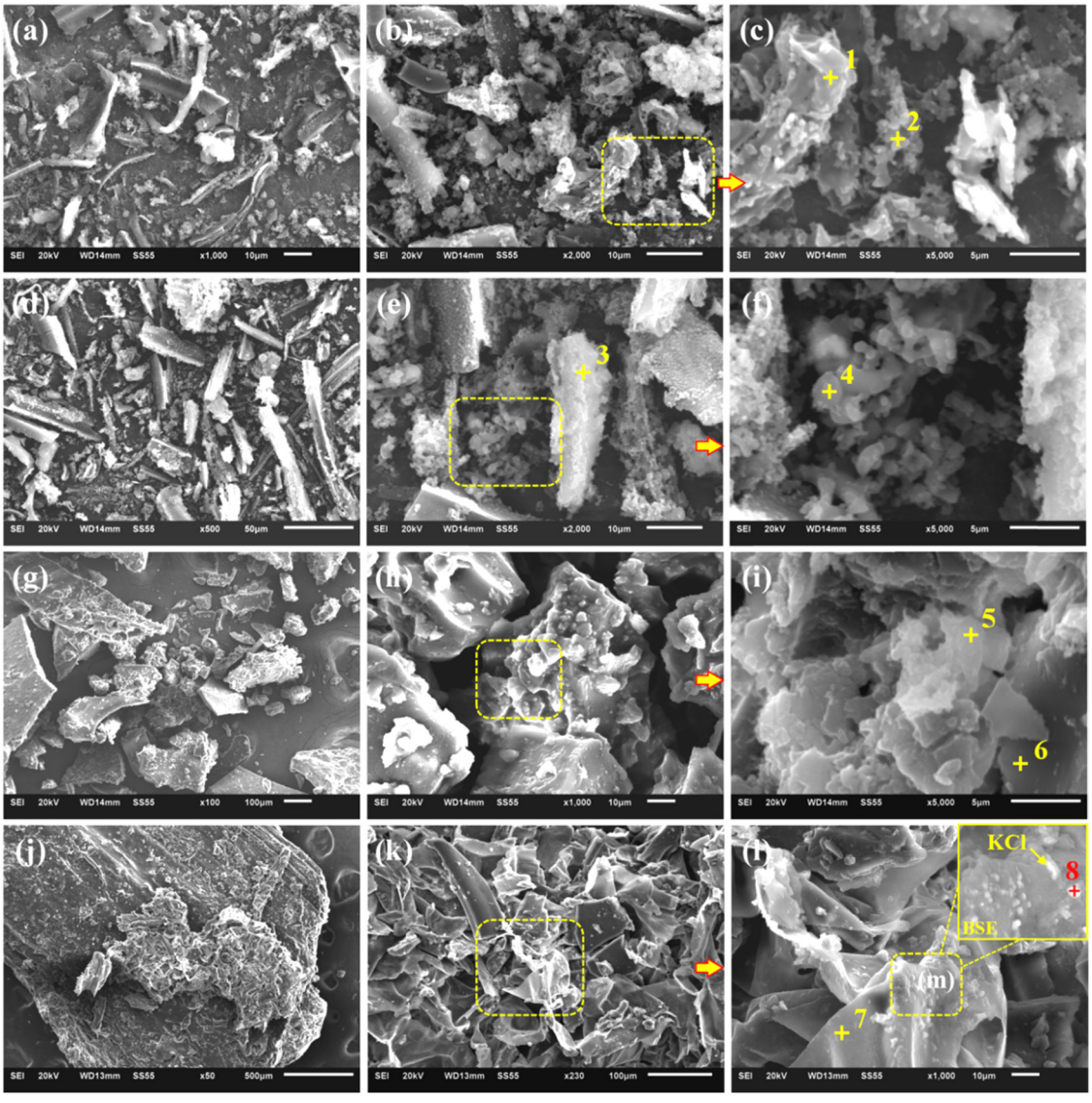

Figure 12: SEM micrographs of corn stalk hydrochars prepared at various mass ratios. (a)–(c) 1%; (d)–(e) 2%; (g)–(i) 3%; (j)–(l) 4%; and (m) high magnification SEM image.

of the granular hydrochars is about 200 nm–2 μm, as shown in the Figure 10(d)–(l). It is worth noting that no white KCl particles are observed in the hydrochars after the carbonization time exceeded 40 min, indicating that the harmful KCl particles had been completely dissolved. It can be seen from Figure 11(a) that increasing carbonization time can significantly increase the carbon content of corn stalk hydrochars and reduce the oxygen content. When carbonization time is 40–80 min, the contents of C and O are 71.87–80.52 wt% and 19.48–27.95 wt%, respectively.

The calorific values of corn stalk hydrochars prepared at different carbonization times are shown in Figure 11(b). It can be seen that under the condition of fixed carbonization temperature and solid–liquid mass ratio, increasing carbonization time can significantly increase the calorific values of corn stalk hydrochars. When the carbonization time is 40–80 min, the calorific values of corn stalk hydrochars is 22.33–23.46 MJ·kg^{-1}, and the maximum calorific value (23.46 MJ·kg^{-1}) is observed under the carbonization time of 80 min, which is very close to the calorific value of anthracite. It can be seen that the evolution of functional groups of raw materials in the hydrothermal process will lead to changes in the content of carbon and oxygen elements, and the fixed carbon content will gradually increase with the increase in HTC time, while the oxygen element will gradually decrease, resulting in a gradual increase in the calorific value of biomass fuel [30]. Furthermore, the combustion properties also become more stable with the increase in carbon content. Therefore, the corn stalk hydrochars have a great potential to replace non-renewable energy sources such as anthracite. Singh et al. [13] also agreed that the emergence of HTC is a sustainable method for converting wet biomass into high value-added biochar and an innovation in waste to energy conversion. In addition to resource substitution, the HTC process may also create more job opportunities in the future to alleviate employment pressure.

3.3.3 Effect of mass ratios

Figure 12 shows the SEM images of corn stalk carbonization products prepared under various solid–liquid proportions, and the EDS elemental components of hydrochars

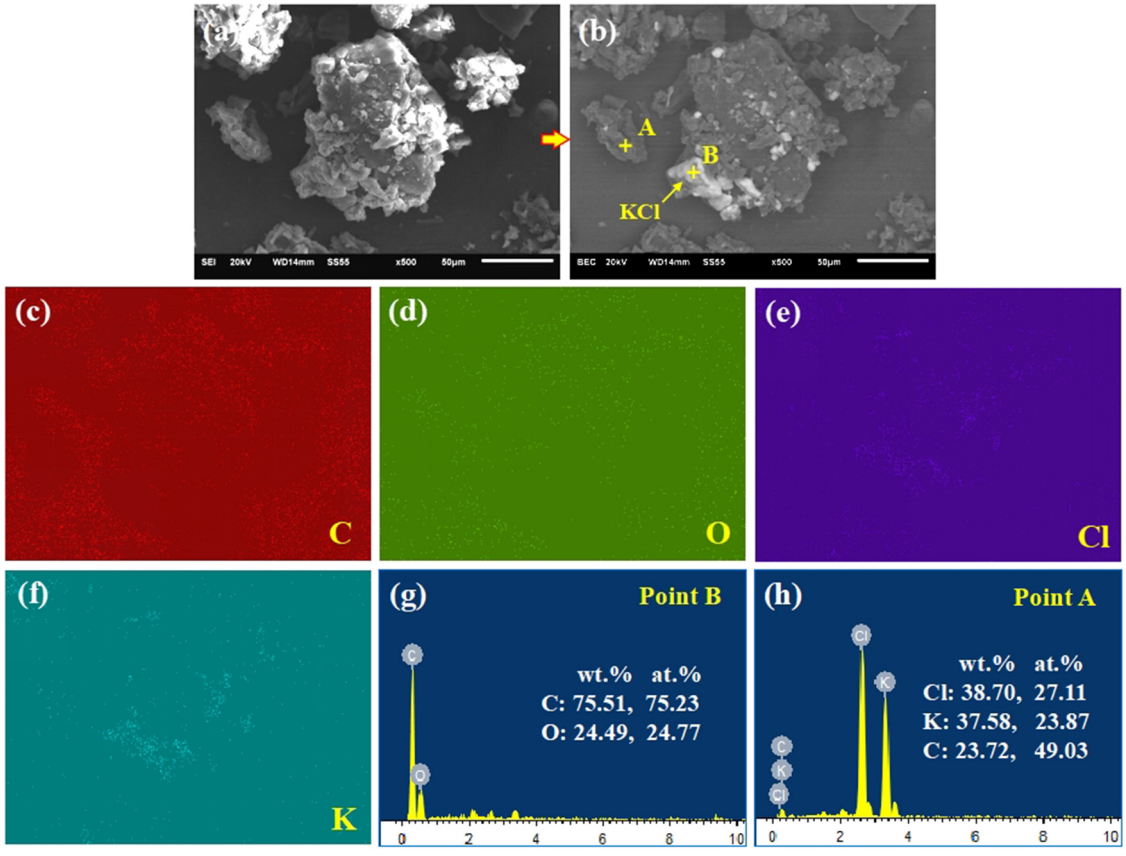

Figure 13: SEM images and EDS elemental analysis of hydrochars prepared at 4% solid–liquid proportions. (a) SEM image; (b) backscattered electrons image; (c)–(f) EDS mapping of C, O, Cl, K elements; (g) and (h) EDS spectrum.

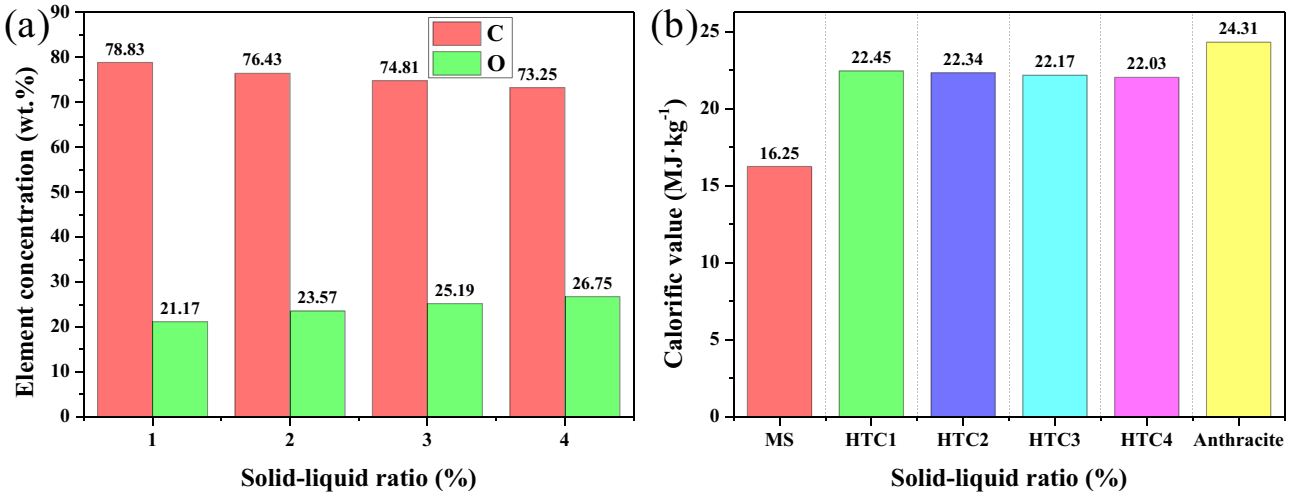

Figure 14: EDS element concentration (a) and calorific value (b) of corn stalk hydrochars prepared at various carbonization mass ratios.

prepared under diverse solid–liquid proportions are shown in Figure 14(b). As shown in Figure 12(a)–(f), when the solid–liquid mass ratio is 1 and 2%, the corn stalks are carbonized into fine particles and strip products with sizes of 0.2–10 μm and 10–60 μm, respectively. This fine porous microstructure greatly improves the reactivity of carbonized products, and has a high carbon content, the content of C element is 75.34–79.45 wt%, and the content of O element is 21.79–24.66 wt%. As shown in Figure 12(g)–(i), when the solid–liquid mass ratio is 3%, the size of the carbonized product significantly increases, and the carbonized product presents a granular and sheet-like structure with a size of about 50–300 μm. The content of C element in the carbonized product slightly decreases, while the content of O element slightly increases. The content of C element is 73.49–76.12 wt%, and the content of O element is about 23.88–26.51 wt%. As shown in Figure 12(j)–(m), the size of the carbonized product reaches the millimeter level under the solid–liquid mass ratio of 4%, and the striped structure of the original corn stalks can still be observed. Some cell walls have undergone carbonization and rupture, with a size of about 100 μm, and obvious agglomeration phenomena can be observed. In addition, the content of C element also slightly decreased (75.61 wt%), and white KCl particles with a size of about 1–3 mm are observed in the microzone (m).

The SEM images and EDS elemental analysis results of carbonized products prepared with a mass ratio of 4% are presented in Figure 13. The carbonized products mainly consist of black phase (hydrochar) and white KCl particles, as shown in Figure 13(b). The EDS element distribution shows that the black hydrochar is mainly composed of C and O elements, and their contents are 75.51 and 24.49 wt%, respectively. The white particle phase is mainly composed of Cl and K elements with a molar ratio of about 1:1, and the Cl and K elements show the same distribution law, which further confirms that the white particle phase is residual KCl. Therefore, although the high solid–liquid proportion can prominently raise the carbonized product yields, it is not favorable for the dissolution of harmful phase KCl. The influence of hydrothermal carbon calorific value under different solid–liquid proportion conditions is shown in Figure 14(b). It can be seen that as the solid–liquid ratio increases, the calorific value of hydrochars slightly decreases with the increase in solid–liquid mass ratio, but it still has a high calorific value (22.03–22.45 $MJ{\cdot}kg^{-1}$). Therefore, when the fixed carbonization temperature is 260°C and the carbonization time is 40 min, the change in solid–liquid mass ratio has little effect on the calorific value of hydrochars.

4 Conclusion

The corn stalk biomass resources are used to prepare renewable biochar through a HTC process. The effects of HTC parameters on phase composition, surface functional groups, microstructure evolution, and the calorific values of the maize stalk hydrochars were measured and analyzed. And the main conclusions are as follows:

(1) The results of XRD analysis indicated that with the increase in HTC temperature and carbonization time, the peak intensity of organic compounds in the carbonized products significantly decreases, and the number of diffraction peaks also significantly decreases.

Meanwhile, the ordered carbon structure of the carbonized products significantly increases, and the degree of graphitization gradually increases. This indicates that increasing the carbonization temperature and time can effectively promote the dehydration and dehydroxylation reactions of corn stalks, promote the decomposition of organic matter, and accelerate the carbonization reaction rate.

(2) The FTIR analysis results showed that the higher the carbonization temperature and time, the lower the peak intensity of hydroxyl groups (−OH), and a significant dehydroxylation reaction occurred between cellulose and hemicellulose. The peak intensity of C–H bonds in fatty hydrocarbons or cycloalkanes slightly decreases with increasing temperature and time, indicating that the $-CH_3$ and $-CH_2$ bonds in corn stalk biomass are relatively stable. In addition, increasing the carbonization temperature and time can promote the decomposition of functional groups, and the easily decomposable aliphatic functional groups gradually weaken or even disappear. It is worth noting that the lower the solid–liquid mass ratios, the better the carbonization effect. A lower solid–liquid mass ratio can also promote the dehydration and dehydroxylation reactions of corn stalks.

(3) The HTC process conditions have a significant influence on the microstructure of corn stalk hydrochars. The higher the carbonization time and temperature, the finer the particle size of carbonization products, and the higher the content of C element and calorific value. Under the carbonization temperature of 260–300°C (t = 40 min, S/L = 2%), the C content and calorific value of corn stalk hydrochars are 72.82–73.61 wt% and 22.36–23.58 MJ·kg^{-1}, respectively. When the carbonization time is 40–80 min (T = 260°C, S/L = 2%), the C content and calorific value of corn stalk hydrochars are 72.70–79.28 wt% and 22.33–23.46 MJ·kg^{-1}, respectively.

(4) The solid–liquid mass ratio also has significant influence on the microstructure and phase composition of corn stalk hydrochar. When the solid–liquid ratio is 1 and 2%, the corn stalk has been carbonized into fine strips and particles under the solid–liquid mass ratio is 1 and 2%, and this fine porous microstructure greatly improves the reactivity of carbonized products. These carbonized products have high carbon content (75.34–79.45 wt%) and calorific value (22.34–22.45 MJ·kg^{-1}), as well as low oxygen content (21.79–24.66 wt%). When the solid–liquid mass ratio is 3%, the size of the carbonized product significantly increases, the content of C element slightly decreases, and the content of O element slightly increases. When the solid–liquid mass ratio is 3 and 4%, the size of the carbonized product significantly increases, the content of C element slightly decreases, and the content of O element slightly increases. It is worth noting that the size of the carbonized product reaches millimeter level under the solid–liquid mass ratio of 4%. In addition, white KCl particles with a size of approximately 1–3 mm are also observed. Although a high solid–liquid ratio can significantly improve the yield of carbonized products, it is not conducive to the dissolution of harmful phase KCl.

(5) Under the optimal carbon process conditions (T = 260°C, t = 40 min, S/L = 2%), the corn stalk hydrochar has a smaller particle size (<50 μm), higher calorific value (22.34 MJ·kg^{-1}), and carbon content (76.46 wt%), which has a great potential to partially replace anthracite and promote the sustainable development of the metallurgical industry.

Acknowledgments: This work was supported by the Distinguished Youth Research Project of Anhui Provincial Universities (No. 2023AH020019) and Open Fund Project of State Key Laboratory of Advanced Steel Process and Materials (No. RZ2300000011).

Funding information: This work was supported by the Distinguished Youth Research Project of Anhui Provincial Universities (No. 2023AH020019) and Open Fund Project of State Key Laboratory of Advanced Steel Process and Materials (No. RZ2300000011).

Author contributions: Z.H. Zhang: investigation, writing – original draft, visualization, and formal analysis. X. Shen: software, conceptualization, methodology, and investigation. Y.Y. Zhang: writing – review and editing, validation, resources, supervision, data curation, and funding acquisition. Zhichen Han: formal analysis, investigation, and conceptualization. G.Q. Zhang and Z.H. Xie: methodology and investigation.

Conflict of interest: The authors state no conflict of interest.

References

[1] Wang, S., C. B. Yin, J. Jiao, X. M. Yang, B. Y. Shi, and A. Richel. StrawFeed model: An integrated model of straw feedstock supply chain for bioenergy in China. *Resources, Conservation And Recycling*, Vol. 185, 2022, id. 106439.

[2] Chen, J. M., C. L. Li, Z. Ristovski, A. Milic, Y. T. Gu, M. S. Islam, et al. A review of biomass burning: Emissions and impacts on air quality,

health and climate in China. *Science of The Total Environment*, Vol. 579, 2017, pp. 1000–1034.
[3] Shi, W. J., Y. R. Fang, Y. Y. Chang, and G. H. Xie. Toward sustainable utilization of crop straw: Greenhouse gas emissions and their reduction potential from 1950 to 2021 in China. *Resources, Conservation and Recycling*, Vol. 190, 2023, id. 106824.
[4] Zhang, Z. H., X. Shen, Y. Y. Zhang, Z. C. Han, and C. Y. Zhang. Effects of hydrothermal carbonization process parameters on physicochemical properties and combustion behavior of maize stalk hydrochars. *Korean Journal of Chemical Engineering*, Vol. 41, 2024, pp. 3035–3051.
[5] Zhang, Y. Y., L. H. Yu, K. K. Cui, H. Wang, and T. Fu. Carbon capture and storage technology by steel-making slags: Recent progress and future challenges. *Chemical Engineering Journal*, Vol. 455, 2023, id. 140552.
[6] Yu, L. H., X. Shen, Y. Y. Zhang, H. L. Liu, C. Y. Zhang, and Z. C. Han. Raw material design, sintering temperature optimization and development mechanism investigation of self-foaming porous bricks with high solid waste addition. *Chemical Engineering Journal*, Vol. 495, 2024, id. 153711.
[7] Zhang, H. F., D. W. Hu, J. M. Chen, X. N. Ye, S. X. Wang, J. M. Hao, et al. Particle size distribution and polycyclic aromatic hydrocarbons emissions from agricultural crop residue burning. *Environmental Science and Technology*, Vol. 45, 2011, pp. 5477–5482.
[8] Zhang, H. F., X. N. Ye, T. T. Cheng, J. M. Chen, X. Yang, L. Wang, et al. A laboratory study of agricultural crop residue combustion in China: emission factors and emission inventory. *Atmospheric Environment*, Vol. 42, No. 36, pp. 8432–8441.
[9] Sun, J. F., H. Y. Peng, J. M. Chen, X. M. Wang, M. Wei, W. J. Li, et al. An estimation of CO_2 emission via agricultural crop residue open field burning in China from 1996 to 2013. *Journal of Cleaner Production*, Vol. 112, 2016, pp. 2625–2631.
[10] Yiin, C. L., E. B. Odita, S. S. M. Lock, K. W. Cheah, Y. H. Chan, M. K. Wong, et al. A review on potential of green solvents in hydrothermal liquefaction (HTL) of lignin. *Bioresource Technology*, Vol. 364, 2022, id. 128075.
[11] Sofian, A. D. A. B. A., H. R. Lim, K. W. Chew, K. S. Khoo, I. S. Tan, Z. L. Ma, et al. Hydrogen production and pollution mitigation: Enhanced gasification of plastic waste and biomass with machine learning & storage for a sustainable future. *Environmental Pollution*, Vol. 342, 2024, id. 123024.
[12] González-Arias, J., M. E. Sánchez, J. Cara-Jiménez, F. M. Baena-Moreno, and Z. E. Zhang. Hydrothermal carbonization of biomass and waste: A review. *Environmental Chemistry Letters*, Vol. 20, 2022, pp. 211–221.
[13] Singh, A., A. D. Bin Abu Sofian, Y. J. Chan, A. Chakrabarty, A. Selvarajoo, Y. A. Abakr, et al. Hydrothermal carbonization: Sustainable pathways for waste-to-energy conversion and biocoal production. *GCB Bioenergy*, Vol. 16, 2024, id. e13150.
[14] Benavente, V., E. Calabuig, and A. Fullana. Upgrading of moist agro-industrial wastes by hydrothermal carbonization. *Journal of Analytical and Applied Pyrolysis*, Vol. 113, 2015, pp. 89–98.
[15] Ischia, G., N. D. Berge, S. Bae, N. Marzban, S. Román, G. Farru, et al. Advances in research and technology of hydrothermal carbonization: achievements and future directions. *Agronomy*, Vol. 14, 2024, id. 955.
[16] Libra, J. A., K. S. Ro, C. Kammann, A. Funke, N. D. Berge, Y. Neubauer, et al. Hydrothermal carbonization of biomass residuals: a comparative review of the chemistry, processes and applications of wet and dry pyrolysis. *Biofuels*, Vol. 2, 2011, pp. 71–106.
[17] Wang, R. K., J. D. Jia, Q. Z. Jin, H. W. Chen, H. T. Liu, Q. Q. Yin, et al. Forming mechanism of coke microparticles from polymerization of aqueous organics during hydrothermal carbonization process of biomass. *Carbon*, Vol. 192, 2022, pp. 50–60.
[18] Pérez, C., J.-F. Boily, S. Jansson, T. Gustafsson, and J. Fick. Acid-induced phosphorus release from hydrothermally carbonized sewage sludge. *Waste and Biomass Valorization*, Vol. 12, 2021, pp. 6555–6568.
[19] Wang, G. W., J. L. Zhang, J. Y. Lee, X. M. Mao, L. Ye, W. R. Xu, et al. Hydrothermal carbonization of maize straw for hydrochar production and its injection for blast furnace. *Applied Energy*, Vol. 266, 2020, id. 114818.
[20] Liu, L. M., Y. B. Zhai, H. X. Wang, X. M. Liu, X. P. Liu, Z. X. Wang, et al. Treatment of sewage sludge hydrothermal carbonization aqueous phase by Fe(II)/CaO_2 system: Oxidation behaviors and mechanism of organic compounds. *Waste Management*, Vol. 158, 2023, pp. 164–175.
[21] Zhang, X. Y., B. Gao, S. N. Zhao, P. F. Wu, L. J. Han, and X. Liu. Optimization of a “coal-like” pelletization technique based on the sustainable biomass fuel of hydrothermal carbonization of wheat straw. *Journal of Cleaner Production*, Vol. 242, 2020, id. 118426.
[22] Kambo, H. S. and A. Dutta. A comparative review of biochar and hydrochar in terms of production, physico-chemical properties and applications. *Renewable and Sustainable Energy Reviews*, Vol. 45, 2015, pp. 359–378.
[23] Sharma, R., K. Jasrotia, N. Singh, P. Ghosh, S. Srivastava, N. R. Sharma, et al. A comprehensive review on hydrothermal carbonization of biomass and its applications. *Chemistry Africa*, Vol. 3, 2020, pp. 1–19.
[24] Sarker, T. R., R. Azargohar, A. K. Dalai, and M. Venkatesh. Physicochemical and fuel characteristics of torrefied agricultural residues for sustainable fuel production. *Energy & Fuels*, Vol. 34, 2020, pp. 14169–14181.
[25] Durmaz, S., Ö. Özgenç, I. H. Boyacı, Ü.C. Yıldız, and E. Erişir. Examination of the chemical changes in spruce wood degraded by brown-rot fungi using FT-IR and FT-Raman spectroscopy. *Vibrational Spectroscopy*, Vol. 85, 2016, pp. 202–207.
[26] Sun, J., X. Sun, H. Zhao, and R. Sun. Isolation and characterization of cellulose from sugarcane bagasse. *Polymer Degradation and Stability*, Vol. 84, 2004, pp. 331–339.
[27] Wang, Z. W., M. G. Wu, G. F. Chen, M. J. Zhang, T. L. Sun, K. G. Burra, et al. Co-pyrolysis characteristics of waste tire and maize stalk using TGA, FTIR and Py-GC/MS analysis. *Fuel*, Vol. 337, 2023, id. 127206.
[28] Yang, H., R. Yan, H. Chen, D. H. Lee, and C. Zheng. Characteristics of hemicellulose, cellulose and lignin pyrolysis. *Fuel*, Vol. 86, 2007, pp. 1781–1788.
[29] Yao, F. Q. and H. H. Wang. Theoretical analysis on the constitution of calorific values of biomass fuels. *Journal of Energy Resources Technology*, Vol. 141, 2019, id. 022207.
[30] Cheng, X. and B. Wang. Influence of organic composition of biomass waste on biochar yield, calorific value, and specific surface area. *Journal of Renewable and Sustainable Energy*, Vol. 10, 2018, id. 013109.
[31] Zhang, X. Y., S. J. Zhu, J. G. Zhu, J. C. Hui, Y. H. Liu, J. H. Zhang, et al. Preheated combustion characteristics and fuel-nitrogen conversion paths for bituminous coal and anthracite in wide-range preheating temperature. *Journal of the Energy Institute*, Vol. 108, 2023, id. 101222.